Low-Temperature Pyrolysis of Brown Coal and Brown Coal Containing Iron Hydroxyl Complexes

ARTICLE *in* ENERGY & FUELS · JULY 2006

Impact Factor: 2.79 · DOI: 10.1021/ef060114h

3 AUTHORS, INCLUDING:

George Domazetis
La Trobe University
43 PUBLICATIONS **803** CITATIONS
SEE PROFILE

Monthida Raoarun
Kasetsart University
6 PUBLICATIONS **111** CITATIONS
SEE PROFILE

Low-Temperature Pyrolysis of Brown Coal and Brown Coal Containing Iron Hydroxyl Complexes

George Domazetis,* Monthida Raoarun, and Bruce D. James

Chemistry Department, La Trobe University, Victoria 3086, Australia

Received March 22, 2006. Revised Manuscript Received June 14, 2006

The concentrations profiles of CO_2 and CO have been measured at 150−600 °C from the pyrolysis, at slow heating rates, of acid-washed brown coal and brown coal containing iron hydroxyl complexes. CO_2 formation was greater at low temperatures, but CO increased relative to CO_2 with an increasing temperature. The ratio CO_2/CO was larger for coal with iron, compared to that from acid-washed coal. The iron species in the chars were Fe_2O_3 at 200−400 °C, Fe_2O_3 and Fe_3O_4 at 400−600 °C, and Fe^0 at 700 °C; inorganic carbonate was also detected. Although conventional chemical kinetic simulations could reproduce the total weight loss of coal with temperature, such calculations could not simulate the measured CO_2 and CO concentration profiles. Decarboxylation reactions may proceed via a number of reaction routes, including ones involving intermediate species. Semiempirical quantum mechanics modeling (SE-QM) of decarboxylation using three carboxylic compounds provided a relative order of decomposition as carboxylic acid ∼ carboxylate ≫ radical. SE-QM and single-point self-consistent field (1scf) calculations, using 2D and 3D models of brown coal, were conducted to provide changes in the heats of formation for models after the loss of carboxyl groups. Such calculations also indicated that hydrogen transfer from a phenoxyl group to a carbanion was energetically favored. The formation of the various iron oxides in coal was modeled by (i) decarboxylation reactions via an iron−carbonato complex decomposing into CO_2 and a μ-oxo iron complex and (ii) decarboxylation of coal via the reduction of iron complexes and the formation of organic radicals.

Introduction

An understanding of the pyrolysis of coal is important because it is the initial process for a number of areas of coal utilization, including coal conversion processes, combustion, and gasification. The variation in chemical and physical characteristics of coal and the number of processes using the various coals has inevitably led to studies of pyrolysis using a large number of experimental methods, in which rates of heating vary from slow to extremely high. Pyrolysis studies often determine the rates of product formation and, from this endeavor, lead us to understand the chemical pathways of pyrolysis that led to those products.[1] Models of coal devolatilization have also involved simple empirical expressions of total mass release, with one or two rate expressions, to more complex phenomenological treatments that endeavor to include details of chemical and physical processes. These processes have been discussed by a number of investigators.[1−8] As a result of the large number of coals and the variable experimental methods, it is extremely difficult to obtain chemical mechanistic insights into pyrolysis encompassing all coals, and this is made more difficult when such studies include inorganics added to coals. A great deal of experimental work has been reported on the formation of gaseous products from acid-washed coals and from coals with inorganic compounds. The pyrolysis and gasification of low-rank coals with added inorganics has included the detection of a number of iron species, such as iron carbides and $Fe^{II/III}$ oxides.[9−20] Detailed studies of the thermal chemistry of simpler carboxylic acids and their salts have also been carried out.[21,22]

* To whom correspondence should be addressed. E-mail: g.domazetis@latrobe.edu.au. Fax: 61-3-9479-1399. Telephone: 61-3-9479-2811.

(1) van Heek, K. H.; Hodek, W. *Fuel* **1994**, *73*, 886−896.
(2) Gavalas, G. R. *Coal Pyrolysis*; Elsevier: New York, 1982.
(3) Howard, J. B.; In *Chemistry of Coal Utilization*; Elliott, M. A., Ed.; Wiley: New York, 1981; p 665.
(4) Solomon, P. R.; Hamblen, D. G.; In *Chemistry of Coal Conversion*; Schlosberg, R. H., Ed.; Plenum Press: New York, 1985; p 121. (b) Serio, M. A.; Hamblen, D. G.; Markham, J. R.; Solomon, P. R. *Energy Fuels* **1987**, *1*, 138. (c) Solomon, P. R.; Hamblen, D. G.; Carangelo, R. M.; Serio, M. A.; Deshpande, G. V. *Energy Fuels* **1988**, *2*, 405−422.
(5) Suuberg, E. M. In *Chemistry of Coal Conversion*; Schlosberg, R. H., Ed.; Plenum Press: New York, 1985; p 67. (b) Suuberg, E. M.; Peters, W. A.; Howard, J. B. *Ind. Eng. Chem. Process Des. Dev.* **1978**, *17*, 37−46.
(6) Chen, J. C.; Niksa, S. *Energy Fuels* **1992**, *6*, 254−264. (b) Stephen Niksa, S. *Energy Fuels* **1994**, *8*, 659−670. (c) Niksa, S. *Energy Fuels* **1996**, *10*, 173−187.
(7) Grant, D. M.; Pugmire, R. J.; Fletcher, T. H.; Kerstein, A. R. *Energy Fuels* **1989**, *3*, 175.
(8) Burnham, A. K.; Oh, M. S.; Crawford, R. W.; Samoun, A. M. *Energy Fuels* **1989**, *3*, 42−55.
(9) Carsky, M.; Kuwornoo, D. K. *Fuel* **2001**, *80*, 1021−1027.
(10) Yamashita, H.; Yoshida, S.; Tomita, A. *Energy Fuels* **1991**, *5*, 52−57.
(11) Lin, S.; Harada, M.; Suzuki, Y.; Hatano, H. *Energy Fuels* **2003**, *17*, 602−607.
(12) Ohtsuka, Y.; Asami, K. *Energy Fuels* **1996**, *10*, 431−435.
(13) Yamashita, H.; Ohtsuka, Y.; Yoshida, S.; Tomita, A. *Energy Fuels* **1989**, *3*, 686−692.
(14) Yamashita, H.; Yoshida, S.; Tomita, A. *Energy Fuels* **1991**, *5*, 52−57.
(15) Yamashita, H.; Tomita, A. *Ind. Eng. Chem. Res.* **1993**, *32*, 409−415.
(16) Tanaka, S.; U-emura, T.; Ishizaki, K.; Nagayoshi, K.; Ikenaga, N.; Ohme, H.; Suzuki, T. *Energy Fuels* **1995**, *9*, 45−52.
(17) Ozaki, J.; Nishiyama, Y.; Cashion, J. D.; Brown, L. J. *Fuel* **1999**, *78*, 489−499.
(18) Shirai, M.; Arai, M.; Murakami, K. *Energy Fuels* **2000**, *14*, 1038−1042.
(19) Murakami, K.; Arai, M.; Shirai, M. *Energy Fuels* **2002**, *16*, 752−755.
(20) Shirai, M.; Arai, M.; Murakami, K. *Energy Fuels* **1999**, *13*, 465−470.

10.1021/ef060114h CCC: $33.50
Published on Web 07/29/2006

The loss of carboxyl and carbonyl groups from coals upon heating to yield CO_2, CO, and H_2O has been examined using x-ray photoelectron spectroscopy (XPS).[23]

Our interest in low-temperature pyrolysis stems from investigations on the catalytic gasification of low-rank coals, particularly, Australian and German brown coal with added sodium or calcium and also added transition-metal species such as iron or nickel hydroxyl species.[24−26] Differentiation between thermolysis of metal complexes and the chemistry that may be attributed to any catalyst species, if present, requires an understanding of the initial molecular structure of the added metal complex and the molecular transformations of the inorganic complex within the coal substrate upon heating. It is necessary, therefore, to relate product formation (such as CO_2 and CO) with the transformation of inorganic species at low temperatures, because these events form inorganic complexes that may be subsequently involved in gasification chemistry.

The chemistry relevant to the pyrolysis of coals is extremely complicated. Thermolytic reactions often involve free-radical or ionic species. Free-radical reactions are ubiquitous for the thermal decomposition of organic compounds, often involving a number of elementary reactions in the overall mechanism, which usually is sufficiently described by the thermodynamics of the endothermic chemistry.[27] Decarboxylation to form CO_2 can proceed via heterolytic or homolytic cleavage of the C−C bond, although heterolytic cleavage is more common under hydrothermal conditions. Heterolysis with the loss of CO_2 appears to occur by a variety of mechanisms, which depend upon the structure of the parent acid and the experimental conditions.[28] Studies of the thermal chemistry for small and well-characterized molecules may be undertaken, but the complexity of the molecular matrix of coal and the nature of the incorporated inorganic species prevents a similar detailed examination of the chemistry for coals. Radical mechanisms may be inferred from electron spin resonance (ESR) studies of brown coal; such studies have shown that increasing the temperature caused the loss of oxygen functional groups and the small concentrations of paramagnetic centers at 300 °C increased at ∼400 °C, reaching maximum radical densities around 550 °C.[29] While studies of the thermal decarboxylation of kerogens indicated that the thermal production of CO may also occur via a radical chain mechanism,[30] the thermal behavior of the well-characterized polymer poly(methacrylic acid) has been reported to form CO_2 and also H_2O, CO_2, and CO by mechanisms that include the formation and decomposition of anhydrides;[31] similar chemistry may produce CO_2 and H_2O from low-rank coals, and this has been considered to lead to cross-linking.[32] Additionally, studies involving the pyrolysis of dicarboxylic acids have shown that decarboxylation occurred primarily by an acid-promoted ionic mechanism, with protonation by a second carboxylic acid.[33] The decarboxylation of dicarboxylic acids with single, double, and triple bonds has been reported to occur via anion species, with a four-member C−C(O)−O−H ring as the gas-phase transition state and a cyclic structure incorporating at least one water molecule in aqueous solution.[33] The decarboxylation of benzoic acids was reported to occur with a marked decrease in the activation energy because of water.[33,34] The chemistry of metal complexes containing organic ligands with carboxyl groups often includes the reduction of the metal center under nitrogen, the formation of inorganic carbonates and oxides, and the formation of gases including CO_2, CO, H_2O, and H_2. Complicated solid-phase thermal reactions have been reported for transition-metal carboxylate salts, producing a variety of solid and gaseous products.[35−39]

Our approach to this complex area has been to examine brown coals with added inorganic species using experimental methods, chemical kinetics simulations, and molecular modeling. The nature of the inorganic species added to brown coals has been studied previously.[24−26] In this paper, we discuss the pyrolysis of acid-washed brown coal and samples containing iron (and adventitious sodium), at low heating rates under an atmosphere of nitrogen. Molecular modeling of small carboxyl acid molecules, considered similar to functional groups found in brown coal, has been used to examine reaction pathways of decarboxylation and has been extended to 2D and 3D molecular models of brown coal.

Experimental Section

Coal. A batch of well-mixed German brown coal containing minimal inherent mineral particles was acid-washed to an ash content of ∼0.1−0.4 wt % (dry basis), and samples containing iron species were prepared from this batch as outlined previously.[24−26] Briefly, iron was added by mixing a known volume of the Fe^{III} solution with a known weight of acid-washed brown coal, and the pH of the coal/solution mixture was adjusted in a stepwise manner, avoiding the formation of iron hydroxide precipitate. The pH values of the mixture and the volume of NaOH used at every step were measured. As a result of using NaOH to adjust the pH, the coal samples contained small amounts of sodium. The coal was filtered off and washed thoroughly with distilled water until the pH of the filtrate remained unchanged. The samples were stored in polystyrene jars.

Analysis. Coal samples were analyzed for C, H, O, N, Cl, S, ash, and moisture by the Campbell Microanalytical Laboratory in the University of Otago, New Zealand. The analytical method used the complete and instantaneous oxidation of the sample by "flash combustion" to convert all organic and inorganic substances into combustion products, under conditions sufficient to completely

(21) Eskay, T. P.; Britt, P. F.; Buchanan, A. C., III *Energy Fuels* **1997**, *11*, 1278−1287.
(22) Dabestani, R.; Britt, P. F.; Buchanan, A. C., III *Energy Fuels* **2005**, *19*, 365−373.
(23) Kelemen, S. R.; Gorbaty, M. I.; Kwiatek, P. J. *Prepr.−Am. Chem. Soc., Div. Fuel Chem.* **1994**, *39*, 31−35.
(24) Domazetis, G.; Liesegang, J.; James, B. D. *Fuel Process. Technol.* **2005**, *86*, 463−486.
(25) Domazetis, G.; Raoarun, M.; James, B. D. *Energy Fuels* **2005**, *19*, 1047−1055.
(26) Domazetis, G.; Raoarun, M.; James, B. D.; Liesegang, J.; Pigram, P. J.; Brack, N.; Glaisher, R. *Energy Fuels* **2006**, manuscript accepted for publication.
(27) Poutsma, M. L. *J. Anal. Appl. Pyrolysis* **2000**, *54*, 5−35.
(28) Gould, E. S. *Mechanism and Structure in Organic Chemistry*; Holt, Rinehart, and Wiston: New York, 1959; chapter 9.
(29) Czechowski, F. *Energy Fuels* **1997**, *11*, 951−964.
(30) Ashida, R.; Painter, P.; Larsen, J. W. *Energy Fuels* **2005**, *19*, 1954−1961.
(31) Lazzari, M.; Kitayama, T.; Hatada, K. *Macromolecules* **1998**, *31*, 8075−8082.
(32) Solomon, P. R.; Serio, M. A.; Despande, G. V.; Kroo, E. *Energy Fuels* **1990**, *4*, 42−54.
(33) Li, J.; Brill, T. B. *J. Phys. Chem. A* **2002**, *106*, 9491−9498; ibid, **2003**, *107*, 2667−2673.
(34) Manion, J. A.; McMillen, D. F.; Malhotra, R. *Energy Fuels* **1996**, *10*, 776−788.
(35) Galwey, A. K.; Jamieson, D. M.; Brown, M. E.; McGinn, M. J. In *Reaction Kinetics in Heterogeneous Chemical Systems Proceedings of the 25th International Meeting of the Societe' de Chimie Physique*; Barret, P., Ed.; Societe' de chimie physique: Dijon, France, July 8−12, 1974.
(36) Music, S.; Ristic, M.; Popovic, S., *J. Radioanal. Nucl. Chem.* **1988**, *121*, 61−71. (b) Bassi, P. S.; Randhawa, B. S.; Jamwal, H. S. *Thermochim. Acta* **1983**, *62*, 209.
(37) L'vov, B. V. *Thermochim. Acta* **2000**, *364*, 99−109.
(38) Hussein, G. A. M. *J. Anal. Appl. Pyrolysis* **1996**, *37*, 111−149.
(39) Abdalla, E. M.; Said, A. A. *Thermochim. Acta* **2003**, *405*, 269−277.

oxidize the coal sample, as described previously.[26] The total ash for coals with high amounts of sodium was determined by heating a known weight of dry coal to 300 °C to remove volatiles, followed by heating to 600−800 °C in air to remove all char. Sodium and iron in the coal and char was also measured by acid extraction and atomic absorption spectrometry (AAS) as previously described.[24,25]

Pyrolysis. Samples consisted of acid-washed coal and coal with known amounts of added iron (a sample of coal containing sodium was also included, to determine any impact sodium may exert on the pyrolysis results). Pyrolysis was carried out using a quartz tube reactor placed inside a Lindberg furnace. A constant flow of nitrogen was maintained with a Cole−Parmer flowmeter (tube N032-15ST calibrated for a flow of 0.0−10.0 mL/min). The flow rate of N_2 was always maintained at 10.0 mL/min. Temperatures were measured using a type J thermocouple and a Digi-Sense Digital thermometer, accurate to ±4 °C. Two sets of experiments were performed to (i) determine the total weight loss of the coal sample at specific temperatures and also the CO_2 and CO concentrations at these same temperatures and (ii) measure the CO_2 and CO concentrations for a specific time−temperature ramp.

The first set of experiments was performed after initially determining the dry weight at 110−120 °C in an atmosphere of nitrogen (the coal was cooled in nitrogen to room temperature prior to weighing). The furnace was heated to a constant temperature (e.g., 150, 200 °C, and so on), and the porcelain crucible containing the weighed coal sample was placed into the furnace and kept at that temperature, while the concentration of gases was monitored periodically every 10−20 min for 300−400 min using a gas cell and the Perkin-Elmer 1720-X Fourier transform infrared spectroscopy (FTIR) instrument. The coal sample was then again cooled under nitrogen and weighed; the temperature of the furnace was increased (usually by 50−100 °C); and the procedure was repeated. Thus, at each temperature of the experiment, the total weight loss and the total concentrations of CO_2 and CO formed were measured.

The second set of experiments was performed with a known weight of coal sample remaining in the tube furnace throughout the measurements of CO_2 and CO. These experiments were carried out by heating the coal sample at a set temperature−time profile. The temperature−time profile was initially measuring for the tube furnace with the quartz tube apparatus but without the coal sample. This was done by placing a thermocouple at the center of the tube furnace, with the same gas flow of N_2, and setting the furnace temperature to predetermined positions. Once these measurements were completed, the furnace was allowed to cool to room temperature and a known weight of coal in a porcelain crucible was placed into the tube furnace. The furnace setting was placed at the predetermined settings; CO_2 and CO gas samples were taken; and their concentrations were measured at given periods using the FTIR gas cell. Once steady state conditions had been achieved, the furnace setting was changed to the next temperature; this was repeated with temperatures increases usually of 50 °C, to a final temperature of between 300 and 500 °C.

Char samples were cooled under nitrogen and stored in a desiccator for elemental analysis, scanning electron microscope−energy dispersive X-ray microanalysis (SEM−EDX), and X-ray diffraction (XRD) studies. Inorganic species on the surface of coal and char samples have been examined using XPS.[24,26] Volatiles produced when heating the coal to >600 °C condense as an oily substance on the cooler walls of the quartz tube. When sufficient amounts of the condensate had formed, they were collected by washing the tube with ethanol, and the FTIR spectrum was recorded for a thin film of the oils formed on a KBr disk under vacuum.

FTIR. Spectra were obtained with a Perkin-Elmer 1720X FTIR spectrometer. CO_2 and CO spectra were recorded in the region of 4000−800 cm^{-1}. The concentration for CO_2 was obtained from calibration graphs based on the area of the peaks from 2394.96 to 2283.3 cm^{-1}, and the concentration for CO was obtained from calibration graphs based on the area of the peaks from 2226.09 to 2047.06 cm^{-1}. Calibration of the FTIR cell was performed by measuring these areas for a certified standard mixture of 2.65 vol % CO and 5.27 vol % CO_2. Standard mixtures of lower concentrations were obtained by mixing a measured flow of the standard CO_2 and CO mixture with a known flow of N_2 and allowing this into the gas cell. Six dilutions were carried out to provide seven concentrations of 0.048−5.270 vol % for CO_2 and 0.024−2.650 vol % for CO. The calibration graph for CO was linear over the concentration range of 0−1.3 vol % in nitrogen ($R^2 = 0.99$), and the CO_2 graph was linear over the concentration range of 0−2.6 vol % ($R^2 = 0.97$). For the CO_2 concentration range of 0−5 vol %, however, some deviation from linearity occurred ($R^2 = 0.93$). The experimental concentration range was 0−1.5 vol % for CO and 0−2 vol % for CO_2, while CO_2 concentrations occasionally peaked at 6vol % for the second set of experiments.

SEM−EDX, XRD, and AAS. Details of these techniques have been given previously.[25,26] Samples were examined using SEM−EDX with a JEOL JSM 840 scanning electron microscope operated at an accelerating voltage of 20 kV with a Link Analytical Pentafet thin window X-ray detector with an energy resolution of 140 eV. C, O, Na, and Fe were measured for coal char powder samples coated with Pt. Detailed examination of palletized chars containing iron was also performed using a sample holder in which a ~6 mm diameter by ~0.2 mm depth hole was made to contain the sample. The sample holder with the char was placed in a Perkin-Elmer hydraulic press at a pressure of 1 ton/m^2 for 2 min and then coated with Pt.

XRD analysis was performed on finely ground samples of the coals and chars with a Siemens Kristalloflex D5000 diffractometer and graphite monochromator over the 2θ analysis range of 4−70° using Cu Kα radiation. XRD peaks were analyzed using Macdiff 4.2.5 software.

Iron and sodium in the treated coal were acid-extracted for analysis by AAS with a GBS 933 spectrometer, for sodium at 589.0 nm and for iron at 248.3 nm.

Chemical Kinetics Simulations. Three chemical kinetics schemes were examined using the IBM CKS package:[40] (i) a devolatilization submodel from a large chemical kinetic scheme developed for brown coal combustion, (ii) a scheme using three−six first-order reactions, in which the activation energies and pre-exponential terms were systematically varied and included all relevant rate data for low-rank coals, in an effort to obtain similar concentration profiles to the measured ones; this scheme included a removal rate to simulate the removal of CO_2 and CO from the reaction vessel by nitrogen, and (iii) a hypothetical reaction scheme using single-step calculations, performed with a spreadsheet, in which three reactants [reflecting three functional groups in coal (R_1, R_2, and R_3)] yielded the products CO_2 and CO; the reaction scheme included a reaction forming an intermediate (Int) prior to yielding the product (e.g., $R_1 \rightarrow Int_1 \rightarrow CO_2$ or CO). A mass balance of reactants and products was always maintained.

Molecular Models. Computer molecular modeling of macromolecules used to study the interactions of inorganic species has been discussed previously,[24,25] and details of the development macromolecules for modeling studies of low-rank coals have been discussed by Domazetis and James.[41] For the present studies, molecular modeling was initially carried out using small organic molecules with carboxyl groups similar to those in the coal molecular models. Semiempirical quantum mechanics calculations involving these small molecules were performed with the Fujitsu CAChe ab initio 5.04 software package using the PM5 Hamiltonian (SE-QM-PM5). The package provides calculations for (a) the

(40) Hinsberg, W.; Houle, F.; Allen, F.; Yoon, E.; Chemical Kinetics Simulator Program version 1.01, IBM Almaden Research Center, 1996. (b) Domazetis, G.; Campisis, A. *Chemical Kinetics of Coal Combustion and Pollution Formation*; Report SO/86/104, Research and Development Department, State Electricity Commission of Victoria: Victoria, Australia, 1986. (c) Domazetis, G.; Campisis, A.; Legg, G.; Skomra, B.; Song, W. *Fly Ash Formation and Sulphation during the Combustion of Brown Coal, Vol 2A: SCOFF—A Code for the Simulation of the Chemistry of Coal Fired Furnaces*; NERDDP End of Grant Report ND/88/046, Research and Development Department, State Electricity Commission of Victoria: Victoria, Australia, 1988.

(41) Domazetis, G.; James, B. D. *Org. Geochem.* **2006**, *37*, 244−259.

potential energy map, (b) the saddle point for a reaction, (c) the transition state, and (d) the reaction path to the products. Although these results were compared where possible with reported experimental results and calculations carried out at a higher theoretical level, here, they were used to obtain an order or trend of the relative rate of decarboxylation for each of the functional groups selected. Because the brown coal samples also contained small amounts of sodium, calculations were also performed on the sodium carboxylates. Similar but fewer calculations were performed using 2D and 3D molecular structures; these were usually carried out after the 2D and 3D molecular structures were optimized using SE-QM and then "locking" the unaffected atoms into the position of the optimized structure, leaving only the relevant portion of the molecule for the reaction path calculations.

Molecular structures used to model brown coal were studied containing 0.47−2.09 wt % of sodium and also ones containing 1.7−7.4 wt % of iron. Numerous 3D molecular structures were initially examined using molecular mechanics and single-point self-consistent field calculations (MM/1scf-PM5) to assess and select structures for further SE-QM-PM5 optimization. Three-dimensional molecular models were optimized using MOPAC2002 at the Australian Partnership for Advanced Computing National Facility (APAC-NF).[42] Structures of coal molecular models with Na^+ were initially optimized using the MOZYME-PM5 routine, and selected structures were optimized also using SE-QM-PM5 to ensure that the heats of formation from both methods were similar for the same models (typically results were within 0.4%).

The 3D molecular model with the lowest total energy and lowest heat of formation was selected as the optimum structure. Upon inspection, however, some of these structures contained very short H···O distances involving adjacent carboxyl groups or a combination of near carboxyl and phenol groups. The structures with unrealistically short hydrogen bonds were rejected, even if they were optimized with lower heats of formation.

The addition of Na^+ introduced changes to the molecular configuration, particularly as additional inorganic atoms were added to the coal molecule. In an attempt to maintain as similar as possible configurations for models containing Na^+ and carboxylate anions, the Na^+ was placed adjacent to the carboxylate. Molecular models containing iron hydroxyl species underwent larger changes because of the numerous coordination bonds, and the final configurations were assessed by using the lowest total energy and heat of formation values, with normal bond lengths and angles, particularly for the iron hydroxyl complexes in the coal model. Where short H···O distances were observed in a molecular model, the positions of the iron atoms and that of the coordination bonds were changed and the structure was again optimized until all bond lengths were within normal values. Calculations began with coal Fe^{III} molecular complexes; these were modified to reflect the loss of particular functional groups; and the resulting structures were optimized again. Modeling was carried out upon the formation of various iron species and compared with the experimentally observed iron species in char.

Results and Discussion

Elemental analysis data for the coal and char samples are shown in Table 1, and sodium and iron are determined by acid extraction in Table 2. Samples were prepared with increasing amounts of iron species (sodium in coal was derived from NaOH used during the addition of iron species). Analysis and characterization techniques have been discussed previously.[26]

Weight Loss and CO_2 and CO Concentration Profiles for Acid-Washed Coal. The vol % of CO_2 and CO in the nitrogen gas stream was obtained using calibration graphs obtained with the FTIR gas cell. Quantification of CO_2 and CO for all pyrolysis experiments was performed after the coal sample was dried to a constant weight at 110−120 °C under nitrogen, and water vapor was not detected in the FTIR spectra. The weight loss from coal samples heated at low temperatures and the distribution of volatiles were similar to those reported for low-rank coals.[8,18,24]

Table 1. Analysis Data as wt % Dry Basis, for Coal and Char Samples (Char at 300 °C; Data, ±0.3 wt %)

sample[a]	% C	% H	% O	% ash	% Na[b]	% Fe[b]
acid-washed coal	64.1	4.3	31.0	0.4		
char (acid washed)	70.1	4.1	25.4	<0.3		
coal + Na	57.9	4.9	33.6	3.3	1.1	
coal + Na	52.1	4.5	34.4	8.3	3.3	
coal + Fe/Na	55.5	4.7	35.1	3.9	0.9	1.7
coal + Fe/Na	51.8	4.3	36.6	6.7	0.4	4.5
coal + Fe/Na	48.1	4.2	35.9	11.3	0.5	7.8
coal + Fe/Na	42.9	4.0	35.4	17.0	1.7	12.4
char + Fe/Na	56.7	3.8	30.2	8.4	1.8	5.9
char + Fe/Na	47.4	3.1	29.5	19.2	1.3	18.3
char + Na	64.1	4.2	26.8	3.9	2.9	

[a] Sulfur and chloride were at the detection limits of ±0.3 wt % of the dry weight of the sample. [b] Values determined by acid extraction (±0.1 wt % dry basis).

Table 2. CO_2/CO Ratio for Acid-Washed Coals with Temperature (Average Deviation in Parentheses)

temp.	150 °C	200 °C	300 °C	400 °C	500 °C
initial	3.1	3.1	3.0	1.4	0.9
final	3.0	3.1	2.9	2.6	2.3
average	3.1 (0.01)	3.1 (0.03)	2.8 (0.1)	1.8 (0.14)	1.4 (0.07)

Tars and oils were not observed at lower temperatures, but small amounts of oils were condensed on the cooler walls of the quartz reactor when the acid-washed coal was heated at and above 600 °C; the FTIR spectra of the gases at this temperature contained peaks because of CO_2, CO, CH_4, and H_2O. The FTIR spectra of these condensed oils provided features similar to those reported for condensed oils from the pyrolysis of Yallourn brown coal at 600 °C: strong aliphatic peaks (C−H) at 2922 and 2843 cm^{-1}, a broad hydroxyl peak (O−H) at 3287 cm^{-1}, a medium carbonyl peak (C═O) at 1697 cm^{-1}, and additional features at 1603, 1510, 1457, 1376, 1280, and 1208 cm^{-1}. The spectra differed from that reported for condensed oils from the pyrolysis of Yallourn coal at 800 °C in that the 1034 and ∼800 cm^{-1} peaks were weak and broad, instead of the strong peaks reported for the Yallourn coal.[43]

The ratio of CO_2/CO, measured over the temperature range of 150−500 °C from the first set of experiments, is shown in Table 2. The initial value is based on the concentrations measured at 10−30 min, after introducing the sample into the furnace, while the final value is based on concentrations measured usually after 120 to 200 min. The initial values varied to a greater extent during the first 10−30 min, but the final concentrations of CO_2 and CO at 50−200 min were relatively constant.

The average value shown in Table 2 was obtained by averaging all CO_2/CO data, with the deviation of the average shown in parentheses.

The concentration profile shown in Figure 1 is similar for all samples and temperatures for the first set of experiments, in that the concentration profiles were higher during the initial period. The trend was toward a lower CO_2/CO ratio with an increase in the steady-state temperature, because of an increase in the CO concentration relative to CO_2.

In the first set of experiments, the coal sample experienced an increase in temperature with time over an initial period of ∼10 min, until it attained a steady temperature. During the initial temperature increase, the amounts of CO_2 and CO were higher

(42) Stewart, J. J. P. MOPAC2002, version 2.5.2, Fujitsu Limited, Tokyo, Japan.

(43) Wornat, M. J.; Nelson, P. F. *Energy Fuels* **1992**, *6*, 136−142.

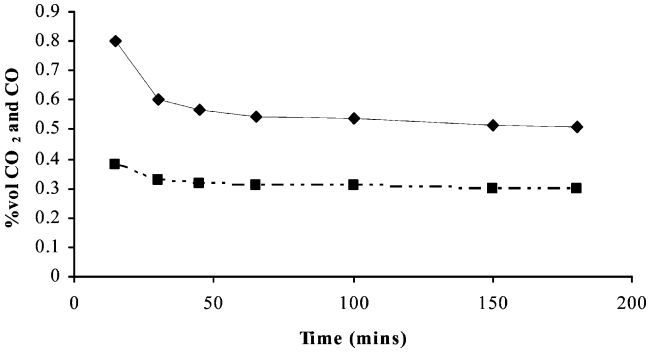

Figure 1. CO_2 and CO (% vol in 10 mL/min of N_2 flow) for aw coal at 300 °C (◆, CO_2; ■, CO).

(as shown in Figure 1). Although the CO_2/CO ratio may be influenced to some extent by any air adsorbed by the sample after weighing, the observed behavior was nonetheless confirmed by the second set of experiments when the sample was not exposed to air. In these, the coal sample remained in the furnace, and data were obtained when the furnace temperature was increased over a ~10 min period and also when the temperature reached a constant value. The data shown in Figure 2 were obtained by heating the coal sample to specific temperatures at various intervals, reaching a final temperature of 400 °C.

The temperature−time profile for the second set of experiments (Figure 2), consisted of a heating period during which the sample underwent an increase in temperature (usually 50 or 100 °C in about 5−10 min), until it reached the constant temperature, and then held constant for a period; this was followed by the next increase in temperature and so on. The data show that the concentrations of gases increased to higher values during the period when the sample experienced an increase in temperature with time and decreased when it reached the constant but higher temperature. Thus, the CO_2/CO ratio varied from 3.1 to 1.6; the variation was now observed when the sample underwent heating with time and also when steady-state conditions were reached. These results differ from the reported increase in the CO_2/CO ratio with temperatures of 150−250 °C for a number of coals of varying ranks, including lignite.[44] The lower amounts of CO_2 formed at higher temperatures, after a lengthy interval, may also be partly due to the depletion of groups that decomposed to CO_2 during the preceding period. These variations in the concentrations occurred with relatively slow rates of heating (usually 10°/min). The increased concentrations of gases during the period of heating from a lower temperature cannot be due to physical factors, such as, for example, diffusion of volatiles through pores in the coal particles, because that should slow the rate of release of gases.

Table 3. CO_2/CO Ratio for Coal Samples with Added Fe Species, with Temperature

coal sample	200 °C	300 °C	400 °C	500 °C
Aw	3.1	3.3	2.9	1.4
Aw + 1.1% Na	3.3	3.4	3	2
Aw + 1.7% Fe (0.1% Na)	2.6	2.7	1.4	
Aw + 4.5% Fe (0.4% Na)	5.9	3.5	1.5	
Aw + 7.8% Fe[a] (0.5% Na)	5.8	4.2	1.4	
Aw + 12.4% Fe[a] (1.7% Na)	5.4	3.5	1.7	

[a] Reproducibility at ~30% of vol % CO_2.

Modeling data (discussed below) in which the loss of carboxyl groups was modeled to form CO_2 and the loss of carbonyl groups was modeled to form CO provided similar cumulative weight losses to the experimental data. Modeling the loss of all carboxyl, carbonyl, ether, and ~40% of phenolic groups, provided a total weight loss at ~44% (similar to the weight loss observed at 600−700 °C). The following data were obtained using molecular models [this may be compared with the experimental elemental composition, CO_2/CO ratios at 300 °C (Tables 1 and 2), and the weight loss for aw coal of 13.6 wt %]. Composition of coal model (molecular weight 4853.7): C, 65.8%; H, 5.0%; O, 28.9%. Composition of char model (molecular weight 4285.6): C, 69.8%; H, 5.6%; O, 24.3%. The weight loss for the model is 12 wt %. The CO_2/CO ratio is 2.8.

CO_2 and CO Concentrations from Coal with Added Inorganics. Table 3 lists the ratio of CO_2/CO for coal containing specific amounts of added Fe (and sodium) from the first set of experiments. While the CO_2/CO ratios in Table 3 differ from those in Table 2, the concentration profiles of gases for coal with added iron were similar to those of the aw coal (Figure 1). The relatively small variation in the CO_2/CO ratio for acid-washed coal containing the relatively high level of 1.1 wt % Na shows that the impact of the small amounts of sodium in coal containing iron was minimal. The reproducibility of the steady-state concentration data for experiments carried out at the same temperature was reasonable for samples with lower amounts of added iron, but the data for coal samples with larger amounts of added iron varied by 30% of the average for both CO_2 and CO concentrations at higher temperatures. The larger CO_2/CO ratio at lower temperatures was due to a greater amount of CO_2 obtained from the coal samples with iron. At higher

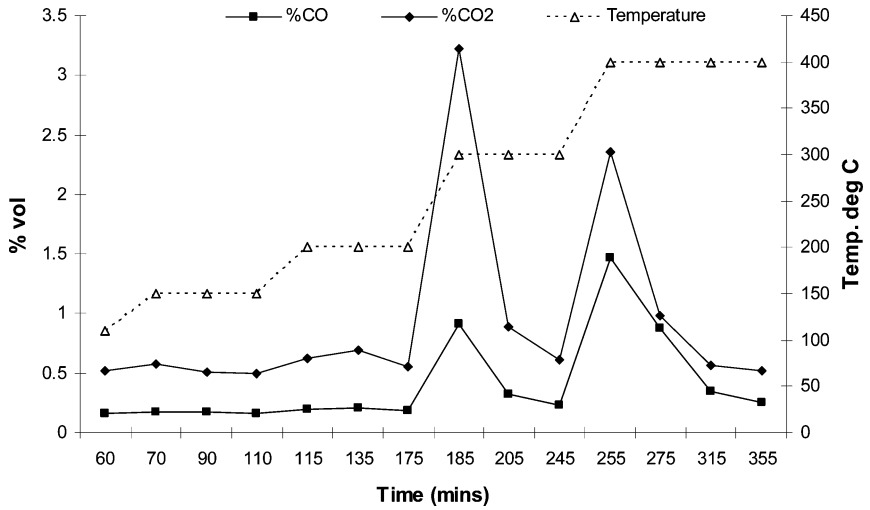

Figure 2. Variation of CO_2 and CO for aw coal (in a N_2 stream) with time and temperature.

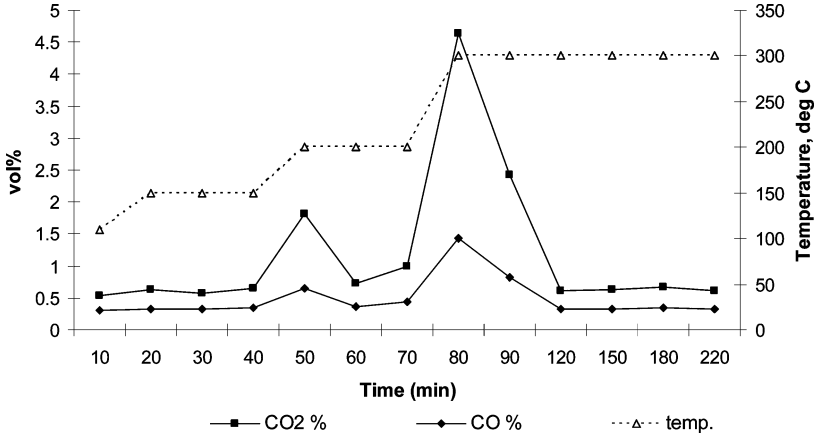

Figure 3. Variation of CO_2 and CO (in a N_2 stream) with time and temperature for coal with 12.4% Fe.

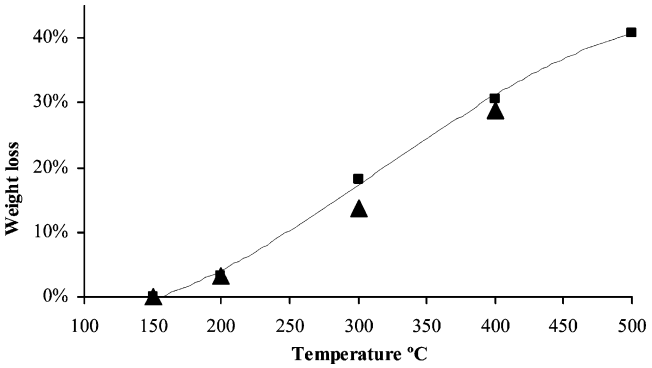

Figure 4. Weight loss of coal with temperature (daf) (coal with 12.4% Fe, ■; acid-washed coal, ▲).

temperatures, however, the CO_2/CO ratio approached that observed for acid-washed coal, because of an increase in the amount of CO. Tars and oils were not observed for the iron and sodium containing coal samples until the temperature was greater than 600 °C. Although a linear correlation could not be found between weight loss nor the CO_2/CO ratio with the variation in the amounts of iron added to the coal, generally under the same conditions, the amount of CO_2 increased with an increase in iron in the coal.

The variation of the concentrations of CO_2 and CO for coal samples containing iron, for the second set of experiments when subjected to a temperature−time profile, was similar to that observed for acid-washed coals. The data for coal containing 12.4% Fe are shown in Figure 3.

The weight loss with temperature for brown coal containing 12.4% iron is shown in Figure 4. This was calculated on a dry ash-free basis (daf) by assuming the ash was Fe_2O_3. Figure 4 also includes data points of the weight loss for acid-washed coal. The initial weight loss would result from decarboxylation reactions. At the higher temperatures, when the weight loss is >20 wt % of the coal, bond breaking would involve additional oxygen function groups, including carboxyl, phenoxyl, ether, and carbonyl. Overall, the weight percent loss profile shown in Figure 4 is similar to that reported for lignites.[6a]

Data from coal models containing iron also show a similar correlation between the decomposition of oxygen functional groups and the experimental values of coal weight loss. It is likely that, with higher amounts of Fe in coal, all of the carboxylate groups (and a number of other oxygen groups in coals) are bound to the iron hydroxyl complexes in coal, and thus, most of the CO_2 and CO would be from the thermal decomposition of iron complexes. At lower Fe concentrations however, only a portion of the carboxyl groups would be bound to the iron hydroxyl species, and the remainder would be bound as carboxyl groups; thermolysis is thus likely to involve a mixture of carboxyl groups chemically bound to iron species and nonbonded carboxyl acid groups. Coal containing relatively large amounts of iron provided an erratic CO_2/CO ratio at higher temperatures, when radical chemistry would predominate.

Iron Species in Char. Iron hydroxyl species added to brown coal have been discussed previously.[26] XRD of chars from coal containing increasing amounts of iron, prepared at temperatures from 200 to 600 °C under nitrogen, exhibited broad peaks identified by XRD as Fe_2O_3 (maghemite-C) and $FeFe_2O_4$ (magnetite). Features attributable to iron carbides were not observed in any of these samples. The XRD of char prepared at 700 °C contained sharp features because of metallic iron and small broad features attributed to maghemite-C. Iron, inorganic oxygen, and carbon, assigned to CO_3, have been reported in the XPS spectra of the surface of these char samples[25,26] and provided binding energy and amount values indicative of iron oxides and carbonate. A specific iron carbonate had not been assigned from the XPS data nor could a crystalline iron carbonate be detected with XRD. Careful examination of these chars using SEM−EDX indicated variable amounts of iron and oxygen within char particles and among the char particles; although the amounts of iron observed varied, the greatest variation in the SEM−EDX was in the amounts of C relative to O. $Na_2CO_3 \cdot xH_2O$ and Na_2CO_3 were identified from the XRD of char samples prepared from coal samples containing only sodium.

Chemical Kinetics of Pyrolysis. Simulations performed using conventional chemical kinetics schemes, including those developed for brown coal (rapid heating rates) could reproduce the overall production of CO_2 and CO at higher temperatures but failed to adequately reproduce the experimentally observed CO_2 and CO concentration profiles shown in Figures 2 and 3.[40] The overall measured weight percent loss of the coal sample could be reproduced using a series of first-order reactions (Arrhenius rate expressions), in which the coal functional groups available for decomposition formed CO_2 and CO. This scheme also provided overall similar CO_2 and CO concentrations to the experimental over 200−500 °C. The scheme consisted of first-order competing reactions for CO_2 and CO formation at 200−400 °C and an additional competing first-order reaction to provide CO at temperatures above 300 °C. In this scheme, the coal was partitioned into two reactants, coal A and B; the relative proportion of coal A reflected the carboxyl groups that would

(44) Karsner, G. G.; Perlmutter, D. D. *AIChE J.* **1982**, *28*, 199−207. (b) Vargast, J. M.; Perlmutter, D. D. *Ind. Eng. Chem. Process Des. Dev.* **1986**, *25*, 49−54.

decompose mainly into CO_2 and a smaller portion of CO at the lower temperature range, and coal B reflected mainly carbonyl and a proportion of ether groups that would decompose into CO at the higher temperatures:

$$\text{coal} \rightarrow \text{coal A and coal B}$$

$$\text{coal A} \rightarrow CO_2, \text{ rate 1;}$$

$$\text{coal A} \rightarrow \text{CO, rate 2 (low temperature)}$$

$$\text{coal B} \rightarrow \text{CO, rate 3 (higher temperature)}$$

The proportion of "coal A" reflected oxygen carboxyl functional groups assumed to decompose at low temperatures into CO_2 at the given rate but could also form some CO at a lower rate; coal B was indicative of oxygen functional groups decomposing into CO at higher temperatures, using the appropriate Arrhenius rate expression. Although this scheme could adequately simulate the overall production of CO_2 and CO, it could not simulate the observed variation in the concentration profiles of CO_2 and CO typically shown in Figures 2 and 3. These observed concentration profiles were qualitatively simulated by performing step calculations, using a hypothetical reaction mechanism involving three reactants $R_{(n)}$, undergoing a sequence of one or two reactions, including the formation of an intermediate $Int_{(n)}$, with a numerically determined rate constant $k_{(n)}$ ($n = 1-3$). Thus, the formation of the products P (CO_2 or CO), with rate constants $k_{(a)}$ or $k_{(b)}$ could be simulated to occur via a one- or two-step mechanism, i.e.,

$$R_{(n)} \xrightarrow{k_{(a)}} P$$

$$R_{(n)} \xrightarrow{k_{(n)}} Int_{(n)} \xrightarrow{k_{(b)}} P$$

This treatment qualitatively simulated the observed concentration profiles for CO_2 and CO. It was not possible to provide a quantitative treatment, and a detailed explanation for these results cannot be proposed at this time. It appears, however, that varying the amounts of the reactants during each sequential step of the reaction scheme, with changes in the reaction rate as the temperature increases (in contrast to a constant temperature), may partly explain why this treatment provided the observed concentration profiles; a mass balance maintained the overall weight loss of the coal during these calculations. This simulation is not intended to provide a unique combination of reaction rates nor a specific chemical reaction scheme. Rather, such a kinetics scheme shows that the observed concentration profiles of CO_2 and CO are due to a number of reactants undergoing differing reactions (discussed below) and are likely to involve intermediate species. As decomposition takes place, the relative concentrations of the functional groups change with time, and as the temperature increases with time, the type of reactions and the reaction rates also change.

Pyrolysis experiments usually provide data by heating a coal sample at a predetermined rate to selected temperatures and measuring the amounts of products formed when the event is quenched; this provides data for phenomenological models. Phenomenological models are typified by simulation packages such as SCCOFF, developed to simulate the chemical kinetics of brown coal combustion,[40a] the functional groups model (FG),[4] FLASHCHAIN,[6] and PERCOLATION.[7] SCCOFF uses a devolatilization submodel consisting of a series of first-order reactions, with the amounts of gases, tar, and char based on the ultimate and proximate analysis of the brown coal. The FG model uses coal containing various chemically identified groups, assumes

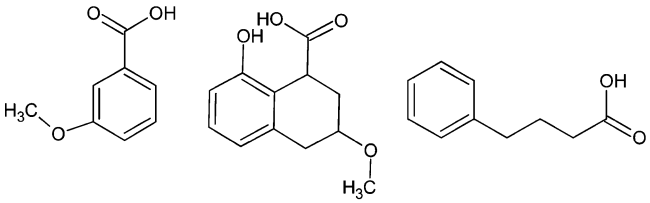

A B C

Figure 5. Molecules used for activation energy calculations.

a mechanism of primary and secondary pyrolysis, and includes the breaking of aliphatic carbon links, arbitrarily chosen as the weakest bridges, to produce molecular fragments, CO_2, light aliphatic gases, CH_4, and H_2O. Radical formation is also invoked to form CO_2, while H_2O is formed by the condensation of two OH groups to produce an ether link. Factors related to the release of CO, CO_2, and H_2O have also been discussed in FLASHCHAIN, which utilizes a four-step reaction mechanism and a population of labile bridges containing the pool of all aliphatic hydrocarbon elements and all oxygen. While the release of CO_2, H_2O, and CO has been treated as one stage, the additional formation of CO at higher temperatures is considered as a separate stage. The PERCOLATION theory has used coal clusters joined by bridges, and it analytically describes the size distribution of discrete coal clusters, assuming that labile bonds may be stipulated and broken during pyrolysis to yield smaller fragments, and nonlabile bonds may also be identified and associated with char formation.

In this paper, pyrolysis has been examined experimentally under relatively non-steady-state and steady-state conditions and with computer molecular modeling of a number of chemical reactions leading to the formation of CO_2 and CO. Molecular models of brown coal have been discussed previously.[25,41] The major products at relatively low temperatures have been CO_2 and CO. The difficulty in elucidating the details of the chemical reactions for coal pyrolysis kinetics has been recognized in large part to be due to the complex organic structures found in coal.[44a]

Molecular Modeling. The rates and extent of decomposition of carboxyl (and other functional groups) will depend upon the chemical nature of these functional groups and their chemical environment, as would the type and amount of products formed (e.g., CO_2, CO, H_2O, H_2, and smaller organic fragments). Carboxyl and phenoxyl functional groups constitute more than half of the oxygen in brown coal, and the remainder is present as carbonyl, methoxyl, ether, and alcohol groups. High CO_2/CO ratios (Tables 2 and 3) are indicative of temperature regions in which decarboxylation chemistry is predominant (150−300 °C).

As the coal molecule(s) undergo heating, the energy provided leads to conformational changes and decomposition reactions. Conformational analysis can be performed for small molecules, but full 1scf-PM5 conformational analysis for all possible large 3D coal molecules, including the formation of intermediates, would require unrealistically large computer resources. Thus, the present modeling is not exhaustive, but it nevertheless shows the likely reaction routes for coal pyrolysis at low temperatures.

Initially, the modeling was of the decarboxylation of the three small molecules shown in Figure 5, representative of the carboxyl functional groups in the coal models. These are three- and four-substituted benzoic acid (A), substituted tetrahydronaphthoic acid (B), and 4-(phenyl)butanoic acid (C), and their sodium compounds. All semiempirical calculations were performed with the PM5 Hamiltonian and are sufficient to provide relative trends based on the calculated activation energies of the particular reactions. The following reactions have been

considered: (i) elimination of CO_2 by the addition of H to the β carbon, (ii) elimination of CO_2 from a carboxylate anion, and (iii) radical elimination of CO_2 or CO.

Low-temperature pyrolysis is assumed to involve mainly carboxylic groups. Although loss of carboxyl groups through anhydride formation and H_2O elimination has also been considered, water vapor has been observed until relatively high temperatures, and this reaction is unlikely to be important at the lower temperatures. Although the major reaction routes at low temperatures involve carboxyl groups, it is likely that other reactions may contribute to product formation but it is assumed the amount is negligible.

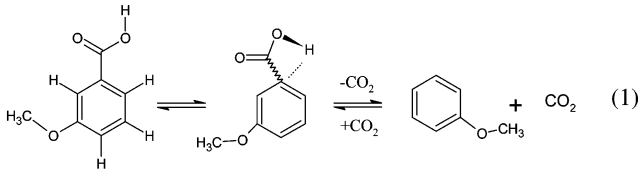

(1)

Calculations for reaction route (i), for (A) and (B) provided similar activation energies. The results obtained for reaction 1 using either three- or four-substituted benzoic acid were sufficiently similar to indicate similar reaction paths. Reported decarboxylation rates for various benzoic acids indicate a dependence on the conditions used for decarboxylation.[22,23,34] Measured activation energies for a series of hydroxyl derivatives of benzoic acid have been reported in the range of 90−97 kJ/mol, but higher theoretical values for these reactions were reported.[33]

Decarboxylation of (B) may be postulated to occur either as in reaction 1 above, or via an intermediate involving the carboxyl H and the phenoxyl H, with proton transfer, as in reaction 2.

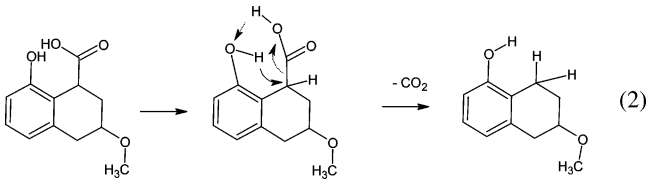

(2)

While the calculated activation energy for (B) and reaction 1 was similar to that for (A), calculations for (B) in reaction 2, involving an intermediate structure, was energetically favored compared to reaction 1. The activation energy for the decarboxylation of 4-(phenyl)butanoic acid (C), however, was considerably larger than for (A) and (B).

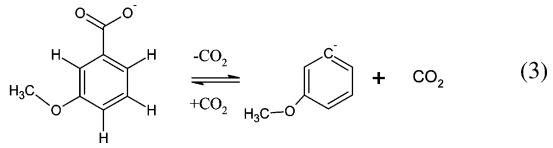

(3)

Calculations for reaction route (ii) provided a relatively large activation energy for reaction 3, which forms a carbanion. Reaction 4 was modeled with the carboxylate anion lost to form the carbanion, followed by the formation of the phenoxide by transfer of H.

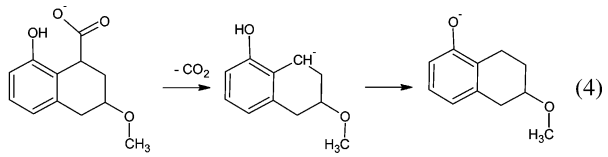

(4)

The modeling results of this reaction sequence indicated the formation of the phenoxide product in reaction 4 was energetically favored, compared to the modeling of only the carbanion formation (as in reaction 3). The activation energy for a similar reaction for compound C was considerably larger, indicating that decarboxylation via this route for this compound was less likely.

Calculations for reaction route (iii) involving radicals is often invoked for the formation of CO_2, H_2, CO, and H_2O [i.e., (R−COOH) → (R˙) + CO_2 + CO + H_2O + H_2]. The formation of H_2 and H_2O is thought to result from radical combination (e.g., H + H → H_2; OH + H → H_2O). Calculations upon radical formation for the compound provided large activation energy (however, radicals present in coal may initiate such a reaction).

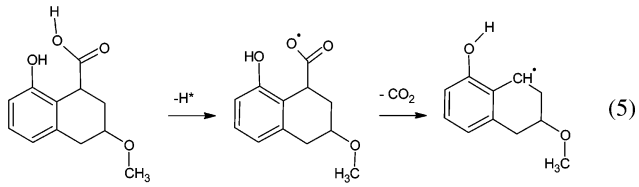

(5)

A larger activation barrier was nonetheless obtained for the loss of CO_2 for reaction 5, compared with reactions 2 and 3. The formation of the oxygen-centered radical was energetically favored by a relatively small amount compared to that for the carbon-centered radical.

Elimination of H_2O and CO_2 via anhydride formation may occur if carboxyl groups were suitably situated in the 3D molecular models of brown coal.

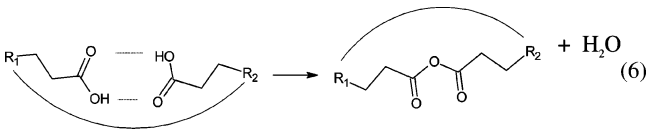

(6)

This reaction has been discussed for poly(methacrylic acid) (PMAD), in which decarboxylation to form CO_2 was assisted by an adjacent acid group and also anhydride and H_2O formation.[31] Adjacent carboxyl groups forming strong hydrogen bonds have been observed in the 3D coal molecular models. It is possible that reaction 6 may contribute to cross-linking reported for coal during heating.[32]

CO may also form by the decomposition of carboxylic, carbonyl, phenolic, and carbonyl groups. Increasing amounts of CO were observed relative to CO_2 at higher temperatures. Decarboxylation calculations of alkyl carboxylic acids, similar to compound C, indicated these would occur at the higher temperatures. Radical reactions often produce a mixture of CO_2 and CO. A possible route to CO formation from carboxyl groups is illustrated by reaction 7, but this reaction requires the almost simultaneous loss of CO and addition of OH.

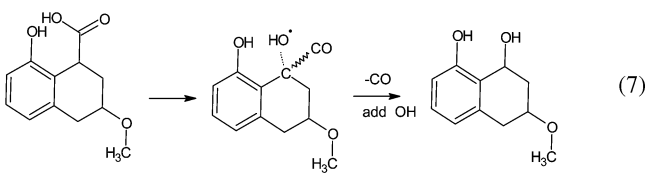

(7)

Pyrolysis of phenols involves phenoxyl radicals that undergo dimerization and also form dibenzofuran.[45] A direct molecular

(45) Wiater, I.; Born, J. G. P.; Louw, R. *Eur. J. Org. Chem.* **2000**, 921−928. (b) Brezinsky, K.; Pecullan, M.; Glassman, I. *J. Phys. Chem. A* **1998**, *102*, 8614−8619.

elimination to CO and C_5H_6 at high temperatures was also considered.[45a] The decomposition of phenol to the cyclopentadiene radical gave a larger activation energy than that for the decarboxylation reactions discussed above, indicating that this route for the decomposition of phenoxyl groups requires higher temperatures. Initial modeling data upon the decomposition of carbonyl groups also provided a larger activation energy, indicating that this chemistry could occur at elevated temperatures to give CO; however, a number of reaction routes and products may need to be considered at these temperatures, including the transfer of H with the formation of a double-bonded alkyl group ($CH_2{=}CH_2{-}R$), formation of radicals and further bond cleavage, or the formation of a new C−C bond.

A number of configurations involving the sodium ion provided significantly different values of the activation energy for the decomposition of the sodium compound of (A). The configuration with Na situated between the methoxyl and carboxylate groups provided the lowest activation energy. Partial charges were consistent with the ionic nature of the compound (Na = +0.56, PhC = −0.44).

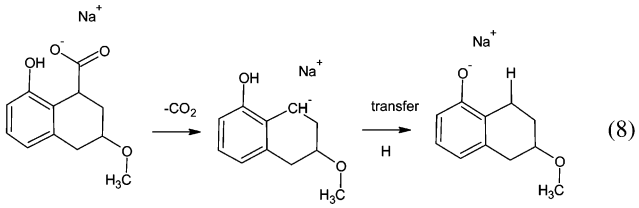

(8)

The chemistry of the sodium carboxylate salt of (B) in reaction 8 includes the transfer of the phenolic hydrogen to the carbanion. H abstraction by methyl radicals from catechol has been reported.[46] Calculations have shown that the phenoxide product is energetically favored over the carbanion, with a moderately low activation barrier for the transfer of H from the phenol group. The activation barrier for the loss of CO_2 from the sodium salt of (B) is similar to that for the sodium salt of (A).

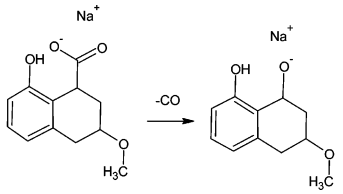

(9)

The activation energy for reaction 9 was somewhat lower than that for the decarboxylation into a carbanion, indicating that CO formation may compete with CO_2 formation for these types of compounds. The activation energy for the decomposition of the sodium salt of (C) into CO_2 was also dependent upon the conformations of the molecule, and although the value was larger than that for the sodium salts of (A) and (B), the calculated activation energy indicated that these type of groups may decompose at moderate temperatures. The reaction of the sodium salt of (C) into CO and the sodium alkoxide was calculated with a similar activation energy to the decarboxylation reaction, but the alkoxide product was more energetically favored compared to the carbanion. Thermal decomposition of sodium, potassium, and calcium salts of octadecanoic acid has been reported to occur at 300−500 °C to give CO (as the major gaseous product) and the inorganic carbonate.[47]

(46) Sun, Y.-M.; Liu, C.-B, *Eur. J. Org. Chem.* **2004**, 120−128.
(47) Rogers, D. E. *Thermochim. Acta* **1984**, *77*, 123−132.

These modeling results indicated that decarboxylation followed the order: carboxylic acid ∼ carboxylate ≫ radical; decarboxylation of acids follow the order: substituted tetrahydronaphthoic ≥ substituted benzoic ≫ straight-chain alkyl.

The 2D and 3D brown coal model contained carboxyl groups similar to those in parts A−C of Figure 4. The weight percent loss for these models has been discussed previously. The weight loss at higher temperatures (as shown in Figure 3) requires the decomposition of almost all carboxyl groups and a significant portion of phenoxyl, carbonyl, and ether groups at temperatures that favor radical mechanisms. Calculations using a 2D molecular model containing carboxyl groups similar to (A) and (B) as sodium carboxylate, provided transition states with similar configurations but with lower activation energies to those of the smaller molecules. Calculations of radical formation, however, gave higher activation energies, but if radicals are naturally present in the coal, this chemistry may occur. The detection of small amounts of CO from the pyrolysis of coal at low temperatures is probably in part due to radicals in the coal; radicals have been reported in low-rank coals, with fairly constant concentrations up to 300 °C, increasing around 400 °C, and reaching maximum values at around 550 °C.[29]

The selection of the optimum configuration for 3D molecular models was based on the lowest heats of formation and total energy and also inspection of bond lengths and bond angles. The extensive hydrogen bonding in these structures provides O···H distances between carboxyl and phenol groups of between 1.9 and 2.2 Å. Some configurations of models containing Na^+ cations and COO^- anions provided a few shorter O···H distances. Although the calculated heats of formation for these various configurations varied by ∼1.5%, structures with very small O···H distances were nevertheless rejected. MOZYME-PM5 optimized 3D coal molecular models, containing sodium cations and carboxyl anions, were modified by removing CO_2 to form a sodium carbanion group ($Na^+\ ^-CR$). This molecular structure was further modified by transferring H from an adjacent phenol group to the carbanion and again optimized. The heat of formation for the model containing the sodium phenoxide was 40 kcal lower than that containing the sodium carbanion. Both conformations of the 3D molecular models were similar, and unusually short hydrogen bonds were not present. A similar trend was obtained for the heats of formation after the loss of one and two CO_2 molecules, with one and two Na^+ in the model, and also for a smaller 3D model containing a total of three Na^+ with the sequential removal of a total of four CO_2 molecules.

Examination of a number of conformations containing sodium and a smaller number containing iron hydroxyl complexes indicates that it may not be possible to make a clear distinction for the decomposition of particular carboxylic groups nor of each of the various mechanisms for decomposition. As conformational changes take place with the increase in temperature, it may be that these changes would favor the decomposition of functional groups that are energetically favored for that molecular conformer. Thus, it is possible that, as the temperature increases, the products formed via the various mechanisms discussed would change.

Molecular Models of Iron(III) Complexes in Coal. Numerous configurations of the 3D coal model molecule with the various iron hydroxyl complexes may be constructed, and an exhaustive analysis of all of them was impractical. The models considered have been discussed previously.[41,25] SE-QM optimization of a molecular model was considered satisfactory if the lowest heat of formation was obtained with bond lengths and bond angles typical for the iron hydroxyl complexes.

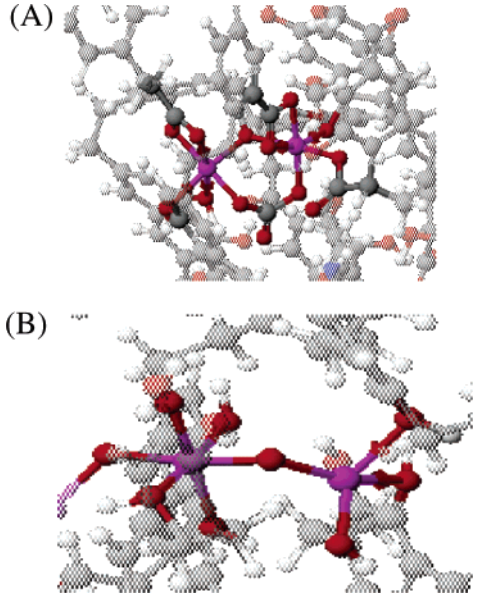

Figure 6. Structures of coal models with (A) iron−carbonato and (B) μ-oxo-$Fe^{III}Fe^{II}$ complexes.

Experimental data have shown that the iron hydroxyl species added to the coal have undergone a series of reactions to form Fe^{III} oxide, a mixture of Fe^{III} and Fe^{II} oxides, carbonate complexes, and finally Fe^0. XRD data identified iron oxides and iron, and inorganic carbon (as CO_3) has been identified by XPS.[25,26] Molecular modeling of brown coal containing iron hydroxyl complexes needs to include the loss of carboxyl groups into CO_2 or CO and the formation of the observed iron oxides. Modeling calculations were carried out for two reaction sequences: (i) the formation of iron−carbonato intermediate complexes that decomposed with the loss of CO_2, to form an iron complex containing a μ-oxo iron bond, and (ii) the loss of CO_2 and CO by bond cleavage, reduction of Fe^{III} to Fe^{II}, and the formation of a radical center. Because the gaseous product observed was mainly CO_2 at lower temperatures, most of this modeling deals with the loss of carboxyl groups as CO_2. Because the C−COO bond is broken, H from the Fe−OH group is transferred, forming an R−CH_3 group. The resulting CO_2··· O−Fe intermediate forms the carbonato complex, resulting in CO_3 acting as a bridging ligand; the CO_3 of the iron−carbonato complex subsequently decomposes into CO_2 and a μ-oxo iron complex. i.e.,

$$\text{coal}[RCH_2(COO)_2Fe(OH)_2Fe(COO)_2R] \rightarrow$$
$$\text{coal}(RCH_3)[(COO)Fe(CO_3)(OH)Fe(COO)_2R] \rightarrow$$
$$\text{coal}(RCH_3)[(COO)(OH)Fe(O)Fe(COO)_2R] + CO_2$$

Carbonato−iron complexes and the loss of CO_2 from these complexes have been reported.[48,49] Figure 6 A illustrates the carbonato complex in a coal model, and Figure 6B illustrates the Fe^{III}/Fe^{II} complex containing a μ-oxo ligand and a tetrahedral Fe^{II} obtained from this model. In the sequence leading to the formation of the μ-oxo complex, one Fe^{III} center becomes five-coordinate following the breaking of the Fe ← OH coordination bond and, subsequently, a phenoxyl group in close proximity forms a additional coordination bond to that iron. The loss of an additional CO_2 could be modeled via the formation of another carbonato complex, in which another carboxyl group bound to iron and a hydroxyl ligand form the next carbonato complex; this would be followed by the loss of the second CO_2, accompanied by the formation of the second μ-oxo bond to the iron centers.

A further loss of a carboxyl group, however, would only occur with the reduction of an Fe^{III} to Fe^{II}. The example in Figure 6A is of the carbonato intermediate $[Fe_2(OH)(CO_3)]^{4+}$, prior to the loss of a CO_2 molecule, for a coal model initially containing $[Fe_2(OH)_2]^{4+}$. The example in Figure 6B is of a coal model initially with $[Fe_3(OH)_6]^{3+}$ that had lost two CO_2 molecules (after the formation of two carbonato complexes), to form the complex with two μ-oxo bonds connecting three iron centers; the reduced Fe^{II} center has formed a tetrahedral structure. Further reactions may occur with an increase in temperature forming H_2O by oxidative formation of an Fe−O−Ph bond (see below). The loss of CO_2 and CO will occur with higher temperatures until Fe^0 is formed. Models are currently being examined upon the formation of char with iron clusters containing reduced Fe centers.

A number of 3D molecular models were examined (SE-QM-PM5 and 1scf-PM5 calculations), containing a variety of iron hydroxyl groups.[41] In these, the initial coal−iron complex model was transformed into the carbonato intermediate and, afterward, into the μ-oxo iron complex after the loss of CO_2. The SE-QM-PM5 and 1scf-PM5 results for the model containing the iron complexes shown in Figure 6A ($C_{172}H_{170}N_2O_{54}Fe_2$; molecular weight, 3240.86. Elemental composition: C, 63.7%; H, 5.3%; N, 0.9%; O, 26.7%; Fe, 3.4%) are as follows: Coal model, coal$[(COO)_4Fe_2(OH)_2]$. SE: total energy, −39 517.92 eV; heat of formation, −2128.08 kcal; partial charges Fe, +1.08 and +1.05. 1scf: total energy, −39 503.90 eV; heat of formation, −1806.11 kcal; partial charges Fe, +1.08 and +1.04. Carbonato complex, coal$[(COO)_3Fe_2OH(CO_3)]$. SE: total energy, −39 517.19 eV; heat of formation, −2111.13 kcal; partial charges Fe, +1.31 and +0.78. 1scf: total energy = −39 504.90 eV; heat of formation, −1827.21 kcal; partial charges Fe, +1.31 and +0.78. μ-oxo-Fe complex, coal$[(COO)_3Fe(\mu\text{-}O)Fe(OH)]$ (loss of CO_2; molecular formula, $C_{171}H_{170}N_2O_{52}Fe_2$). SE: total energy −38 837.99 eV; partial charges Fe, +1.15 and +0.83. 1scf: total energy −38 822.20 eV; partial charges Fe, +1.01 and +0.98.

In this example, the change in the heat of formation for the carbonato complex (compared to the initial coal model) is ∼17 kcal from SE-QM-PM5 and ∼21 kcal from 1scf-PM5. The loss of CO_2 and the formation of the μ-oxo-Fe complex results in a model with a 1.7% increase in the total energy compared to the initial model. A series of 1scf-PM5 calculations, for a model undergoing a sequential loss of $4CO_2$ molecules, provided a linear change in the heat of formation with each additional CO_2, indicating CO_2 may be continuously lost with the formation of carbonato intermediates. Although it is not possible to discuss all of the modeling data, it is clear that eventually all Fe^{III} centers may be reduced via this decarboxylation mechanism, initially forming Fe^{II} and ultimately a mixture of Fe^{II} and Fe^0.

A great deal of data is available in the literature on the thermal chemistry of metal carboxylates, including iron complexes.[35−39] Experimental data of the solid-phase thermal decomposition of the various transition-metal carboxylates needs to be interpreted with care; the decomposition of basic iron acetate has been reported to commence at 200 °C under nitrogen to give Fe_3O_4 at ∼300 °C.[50] Gaseous products have usually been mixtures of CO_2, CO, H_2O, and light hydrocarbons; the decomposition of

(48) Jameson, D. L.; Xie, C.-L.; Hendrickson, D. N.; Potenza, J. A.; Schugar, H. J. *J. Am. Chem. Soc.* **1987**, *109*, 740−746.

(49) Daigaard, P.; McKenzie, C. J. *J. Mass Spectrom.* **1999**, *34*, 1033−1039.

(50) Pinheiro, E. A.; Filho, P. P. A.; Galembeck, F.; Correa da Silva, E.; Vargas, H. *Langmuir* **1987**, *3*, 445−448.

iron octadenoic acid gave CO_2, with the maximum rate of CO_2 evolution observed at 310 °C and the solid products being Fe_3O_4, FeO, Fe, and Fe_3C.[51] The decomposition of Fe^{III} polyacrylate and poly(*meta*)acrylate provided H_2O at 174 and 200 °C, respectively, by anhydride formation; reactions between Fe−OH and carboxylic acid also gave CO_2, CO, and lower hydrocarbons with increased temperature and also mixed iron oxides with the reduction of iron oxides above 600 °C.[52] A detailed study of the decomposition of iron formate concluded that a mixture of ferric and ferrous oxides had formed. The observed ratio of CO_2 and CO was used to assess the extent of reduction of the iron formate to Fe^{II} oxides.[53] ESR signals have also been reported for iron centers and also organic radicals, during the pyrolysis of brown coal with added iron compounds.[18]

SE-QM-PM5 and 1scf-PM5 calculations were also carried out on 3D molecular models of brown coal in which CO_2 was removed, and either an alkyl or aryl carbon-centered radical formed, depending upon the carboxyl group being removed. Subsequent calculations were performed either on a model formed by (i) the elimination of H to form a C═C double bond or (ii) H abstraction by the carbon radical from a suitably situated phenoxyl group [configuration similar to the carboxyl compound (B) discussed previously], to form a phenoxy radical. Calculations for these changes were carried out with coal models containing mono-, di-, and trinuclear iron hydroxyl species. The 1scf-PM5 data for the model coal[$(COO)_2Fe(OH)$], upon forming a coal model with a C or O radical, provided an increase of 1.8% in the total energy compared to the initial model, consistent with an endothermic reaction; the subsequent H elimination to form a carbon double bond was energetically favored by a small amount. The partial charge for Fe^{III} in the initial model was +1.02 and was reduced to Fe^{II} of +0.71 for the coal model containing the radical and +0.74 for the model with the carbon double bond. Similar calculations for the coal model containing a dinuclear iron complex $[Fe_2(OH)_2]^{4+}$ also provided an increase of 1.8% in the total energy after the loss of CO_2; the heat of formation values favored a carbon-centered radical over the formation of a phenoxy radical by H abstraction; the partial charges on the iron centers were +1.09 and +1.04 for the initial model, and after the loss of CO_2 and the reduction of one Fe^{III} to Fe^{II}, partial charges were +0.82 and +0.57 with a carbon radical and +1.06 and +0.57 with a phenoxy radical.

The formation of CO and H_2O could also be modeled by the breakdown of a carboxyl group bound to Fe into CO and the formation of a hydroxyl group bound to the iron center and a carbon double bond (i.e., [coal(H_2C═CH_2)]). This reaction is more likely for alkyl-bonded carboxyl groups at higher temperatures.

$$[(\text{coal})-CH_3-CH_2-C(O)-O-Fe-(O-\text{coal})] \rightarrow [(\text{coal})-CH_2{=}CH_2\ HO-Fe-(O-\text{coal})] + CO$$

The reaction between a phenoxyl OH may then occur to form H_2O and a (Ph−O−Fe) bond (these functional groups are assumed to be part of the coal matrix and in close proximity).

$$[(\text{coal})-Ph-OH + HO-Fe-(O-\text{coal})] \rightarrow [(\text{coal})-Ph-O-Fe-(O-\text{coal})] + H_2O$$

The FTIR spectra of gases obtained at >600 °C show features because of CO_2, CO, CH_4, H_2O, and small amounts of oils and tars (H_2 cannot be detected by FTIR). It is likely that many reactions occur at the higher temperatures; the CO and H_2O formation reaction above illustrates one of a number of possible reaction routes. Work is continuing on pyrolysis and gasification studies and the chemistry of iron species, using a fluidized bed laboratory reactor with the capability to obtain and quench samples of char and analyzing gases using FTIR and gas chromatography, under selected conditions.

Conclusions

The CO_2 and CO concentration profiles from the low-temperature pyrolysis of acid-washed brown coal and coal with added iron reach higher values when the coal underwent an increase in temperature with time than at the final steady temperature. The CO_2/CO ratios were dependent upon the rates of heating and the final temperature of the coal samples, decreasing with an increase in temperature. SE-QM computer molecular modeling has shown that a variety of decarboxylation reactions may occur with differing activation energies; additionally, hydrogen transfer from phenoxyl groups to carbanions has been shown to be energetically favored. Calculations for small organic molecules typical of carboxyl groups in brown coal provided the following order of decarboxylation: carboxylic acid ∼ carboxylate ≫ radical; and the relative ease for decarboxylation follows the order: substituted tetrahydronaphthoic ≥ substituted benzoic ≫ straight-chain alkyl.

1scf and SE-QM calculations indicated that conformational changes to brown coal molecules are an important factor in the overall decomposition, because changes to the configuration of these large molecules may cause changes in the routes for the decomposition of the various oxygen functional groups in brown coal. Thus, it is unlikely that the formation of CO_2 and CO would proceed via separate and distinct reaction routes.

Pyrolysis of brown coal containing iron (and sodium) at low temperatures formed CO_2, CO, and Fe_2O_3; a mixture of Fe_2O_3 and Fe_3O_4 was observed at 300−600 °C, and Fe^0 was observed at 700 °C. SE-QM modeling of coal molecules containing iron hydroxyl species showed that two reaction routes could account for the observed iron compounds: (i) decarboxylation via a carbonato−iron intermediate that decomposed into CO_2 and formed a μ-oxo iron complexes, with additional formation of CO_2 accompanied by the reduction of Fe^{III} to Fe^{II}, and (ii) the breakdown of a carboxyl group into CO_2 or CO to form a carbon-centered radical, with the reduction of Fe^{III} to Fe^{II}. Subsequently, the formation of the C═C double bond in the coal molecular matrix may occur because of the elimination of hydrogen and/or the abstraction by the carbon radical of a hydrogen from a phenoxyl group. At higher temperatures, further reduction of the iron oxide complexes occurs.

Acknowledgment. We gratefully acknowledge Dr. Robert Glaisher, Department of Applied Physics, for SEM−EDX and XRD, Dr. Narelle Brack and Dr. John Liesegang, Centre for Materials and Surface Sciences, for XPS, the Australian Partnership for Advanced Computing National Facility for computer resources under the Merit Allocation Scheme, and the Victorian Partnership for Advanced Computing for a grant and access to computer molecular modeling resources. Rheinbraun GBT kindly supplied samples of German brown coal.

EF060114H

(51) Seddon, A. B.; Wood, J. A. *Thermochim. Acta* **1987**, *118*, 235.
(52) Sileo, E. E.; Morando, P. J.; Baumgartner, E. C.; Blesa, M. A. *Thermochim. Acta* **1991**, *184*, 295−303.
(53) Morando, P. J.; Piacquadio, N. H.; Blesa, M. A. *Thermochim. Acta* **1987**, *117*, 325.